Annals of Nuclear Medicine (2024) 38:288–295
https://doi.org/10.1007/s12149-023-01898-x

ORIGINAL ARTICLE

Performance of ^{99m}Tc-PYP scintigraphy in the diagnosis of hereditary transthyretin cardiac amyloidosis

Honghui Guo[1] · Sha Wu[2] · Xin Xiang[1] · Shuai Wang[2] · Zhihui Fang[1] · Qianchun Ye[1] · Yao Zou[1] · Yunhua Wang[1] · Daoquan Peng[2] · Xiaowei Ma[1]

Received: 12 November 2023 / Accepted: 27 December 2023 / Published online: 22 January 2024

Abstract

Objective Most reported research has primarily investigated wild-type transthyretin cardiac amyloidosis (ATTRwt-CA). However, the application of bone scintigraphy for hereditary transthyretin cardiac amyloidosis (ATTRv-CA) has not been systematically investigated. Therefore, in this study, we aimed to evaluate the diagnostic value of ^{99m}Tc-PYP scintigraphy in ATTRv-CA.

Methods Fifty-four patients were enrolled in a highly suspected cardiac amyloidosis cohort. Transthyretin (TTR) gene characteristics were summarized in the ATTRv-CA group. In ^{99m}Tc-PYP scintigraphy, the diagnostic efficiency of the visual score (VGS) and heart-to-contralateral chest (H/CL) ratio were evaluated. Furthermore, the interobserver consistency among the diagnosticians was investigated.

Results Twenty-eight patients were diagnosed with ATTRv-CA with eight genotypes. The Ala97Ser genotype accounts for 46% ($n=13$) with a mean age of disease onset, definite diagnosis, and interval of 61.6 ± 1.9, 66.5 ± 1.3, and 4.0 (3.0, 6.2) years, respectively. Their VGS is Grade 3, and their H/CL ratio is higher than that of the non-Ala97Ser group, but no statistical significance exists (mean H/CL: 1.95 ± 0.06 vs. 1.87 ± 0.02, $p=0.844$). Additionally, ATTRv-CA patients showed VGS ≥ 2, and mean H/CL ratio of 2.09 ± 0.06. The sensitivity and specificity of VGS were 100% and 65%, respectively. And the interobserver consistency analysis of VGS showed the intraclass correlation coefficient is 0.522. The best cutoff value of H/CL ratio was 1.51 (AUC = 0.996), and the diagnostic consistency of H/CL (bias: 0.018) was high.

Conclusions Ala97Ser is the most common genotype in ATTRv-CA in our cohort, with characteristics of later onset and rapid progression, but delayed diagnosis and extensive ^{99m}Tc-PYP uptake. Overall, ATTRv-CA patients showed moderate-to-extensive myocardial ^{99m}Tc-PYP uptake. Additionally, VGS carries subjectivity, low specialty and interobserver consistency. But H/CL exhibit high diagnostic efficacy and interobserver consistency. The H/CL ratio is more useful than VGS.

Keywords ^{99m}Tc-PYP · Hereditary transthyretin cardiac amyloidosis (ATTRv-CA) · Ala97Ser gene mutation · Single-photon emission computed tomography · Semiquantitative parameter

✉ Yunhua Wang
wangyunhua0801@csu.edu.cn

✉ Daoquan Peng
pengdaoquan@csu.edu.cn

✉ Xiaowei Ma
maxiaowei@csu.edu.cn

Honghui Guo
guohonghui2021@163.com

[1] Department of Nuclear Medicine, The Second Xiangya Hospital, Central South University, Changsha 410011, Hunan, China

[2] Department of Cardiovascular Medicine, The Second Xiangya Hospital of Central South University, Changsha 410011, Hunan, China

Introduction

Transthyretin amyloid cardiomyopathy (ATTR-CA) is caused by the destabilization of the transthyretin (TTR) protein, which promotes release and accumulation of monomers and the formation of amyloid fibrils deposited in the myocardium[1], leading to diastolic dysfunction, arrhythmias, and clinical heart failure[2]. ATTR-CA includes two subtypes: wild-type transthyretin amyloid cardiomyopathy (ATTRwt-CA) and hereditary transthyretin amyloid cardiomyopathy (ATTRv-CA), with the median survival from diagnosis being 3–5 years under untreated conditions [3]. As a rare autosomal-dominant (AD) multisystem disorder [4],

ATTRv-CA has attracted multidisciplinary attention with the application of several novel medicines and the development of diagnostic tools [5]. More than 140 TTR gene mutant forms have been identified, most of which are caused by point mutations. The gene mutation subtypes are diverse, clinical phenotypes are different, and the onset age is varied [5, 6]. Therefore, highlighting the diversity of mutated genotypes is important in revealing the distinct natural histories of diseases, providing insight into likely disease progression and assessing the possibly involved systems and organs [7].

The gold standard for diagnosing ATTR-CA is endomyocardial biopsy (EMB) [8]. However, the small number of medical institutions qualified for EMB, high cost, and low willingness of patients to take the risk of invasive examinations limit the routine application of EMB in the clinic [1]. The increasing evolution of auxiliary diagnostic tools has promoted the diagnosis of cardiac amyloidosis in noninvasive ways. In particular, the dramatic growth of nuclear medicine has made the era of noninvasive diagnosis of myocardial amyloidosis a reality. Reports have confirmed that bone scintigraphy identifies ATTR-CA with high sensitivity and specificity, making the positive predictive value for ATTR-CA reach 100% with the exception of light-chain cardiac amyloidosis (AL-CA) [9–11]. Currently, bone scintigraphy [with ^{99m}Tc-pyrophosphate (PYP), ^{99m}Tc-3,3-diphosphono-1,2-propanodicarboxylic acid (DPD), or ^{99m}Tc- hydroxymethylene-diphosphonate (HMDP) as a tracer] has been recommended to diagnose ATTR-CA in multiple guidelines and expert consensus papers [12–14].

Whereas the most reported research has primarily investigated wild-type ATTR-CA (ATTRwt-CA), the use of bone scintigraphy for ATTRv-CA, especially the gene mutation subtypes, has not been systematically investigated. Accurate noninvasive specific imaging would considerably improve the early diagnosis of ATTRv-CA, facilitate genetic testing and evaluation of the inherent risks of family members [15], and further benefit patient outcomes with early treatment [8, 16]. Therefore, the purpose of our study was to determine the variety of transthyretin (TTR) gene mutations in our center and investigate the diagnostic accuracy of the visual score and semiquantitative parameter (H/CL ratio) of bone scintigraphy (with ^{99m}Tc-PYP as a tracer) in the diagnosis of ATTRv-CA.

Materials and methods

Study population

Eighty patients recommended to undergo ^{99m}Tc-PYP SPECT imaging for possible ATTR-CA at the Second Xiangya Hospital from June 2020 to March 2023 were initially reviewed. They were highly suspected to have ATTR-CA, with typical imaging features of CA on echocardiography and exclusion of AL-CA through negative monoclonal protein testing by serum protein electrophoresis and serum free light chains. The inclusion criteria were as follows: (1) patient was subjected to ^{99m}Tc-PYP SPECT scintigraphy; (2) biopsy was performed; and (3) gene testing was conducted. According to consensus guidelines [14, 17], patients were diagnosed with ATTR-CA by the following criteria: a. extracardiac biopsy-proven ATTR amyloidosis; b. typical cardiac imaging features of CA; c. negative monoclonal protein testing with serum protein electrophoresis and serum-free light chains. Patients were considered to have ATTRv-CA (the ATTRv-CA Group, $n=28$) if ATTR-CA patients had a positive TTR gene test result. ATTR-CA patients with negative TTR gene test results were categorized as ATTRwt-CA ($n=5$). Patients were considered to have no CA (the non-CA group, $n=26$) if they met the following criteria: negative extracardiac biopsy for amyloidosis and TTR gene test; ATTRwt-CA and other patients who did not undergo ^{99m}Tc-PYP scintigraphy, biopsy, or gene testing were excluded from this study. All data were retrieved from the database. This study was conducted with the approval of the Second XiangYa Hospital of Central South University Institutional Review Board (No. 2021162).

^{99m}Tc-PYP SPECT imaging

Seventy-three patients had subsequently undergone a standard imaging protocol with ^{99m}Tc-PYP imaging at 1 h after injection [18]. ^{99m}Tc-PYP scintigraphy was performed using dual-headed single-photon emission computed tomography (SPECT, Philips Skylight, USA). All patients were intravenously administered approximately 555 MBq (15 mCi) of ^{99m}Tc-PYP. Then, imaging was acquired at 1-h postinjection. Anterior and lateral planar images were acquired for 750 K counts using a 256×256 matrix with a 1.5 zoom factor, and the energy window was set at 141 keV ($\pm10\%$) with low-energy high-resolution (LEHR) collimators. Following planar imaging, SPECT imaging was obtained with step mode for 20 s per projection (40 projections per detector, a total of 180° of data).

Imaging was graded by two board-certified and experienced readers (ERs) of the department of nuclear medicine using the visual score and semiquantitative parameter in the planar scans and confirmed in SPECT [19]. The semiquantitative parameters were determined by the average of two experts. The third expert made the final judgment when the two ERs disagreed. In addition to the ERs mentioned above, images were reviewed by another green-hand and inexperienced reader (IR) to verify the interobserver variability of the visual score and semiquantitative parameter among diagnosticians.

The visual score was graded 0–3 using both anterior and lateral planar imaging [8, 20], with 0 as no myocardial uptake, 1 as myocardial uptake less than ribs, 2 as myocardial uptake equal to ribs, and 3 as myocardial uptake greater than ribs with mild or absent rib uptake. For semiquantitative analysis in planar images, the circular region of interest (ROI) was drawn over the heart, which was copied and mirrored to the contralateral chest, and the heart-to-contralateral (H/CL) ratio was calculated based on the mean counts of the ROIs [21].

Biomarkers and echography

Patients were systematically evaluated at our center within 2 weeks of diagnosis. Evaluations consisted of a complete clinical history and examination, alongside functional, biochemical, electrocardiography, and echocardiographic assessment. National Amyloidosis Center (NAC) staging was performed for ATTRv-CA patients [22].

Statistical analysis

All statistical analyses were performed using SPSS statistical software version 26 (IBM Corporation, Armonk, New York). Descriptive statistics were computed to summarize the data. Continuous variables are expressed as the mean ± SD, nonnormal variables are presented as medians with interquartile ranges, and categorical or ordinal variables are presented as frequencies (percentages). Differences between the two groups were compared using Student's test for normally distributed continuous variables or the Mann−Whitney *U* test for nonnormally distributed continuous variables. The $\chi 2$ test was used for comparing groups for categorical variables. Receiver operating characteristic (ROC) curve analysis was applied to assess the diagnostic efficiency of H/CL ratio. Additionally, the kappa value was calculated to verify the interobserver variability of the visual score, and Bland−Altman analysis was used to assess the interobserver variability of H/CL ratio in ^{99m}Tc-PYP scintigraphy. Linear relationships between H/CL ratio and echocardiography or blood biomarkers were evaluated with Pearson correlation coefficients. A two-sided P value < 0.050 was considered statistically significant.

Results

Demographic characteristics

According to the inclusion and exclusion criteria, 54 patients were ultimately enrolled, including 28 ATTRv-CA (the ATTRv-CA group) and 26 non-CA patients (the non-CA group) (Fig. 1). The demographic, clinical, and ^{99m}Tc-PYP scintigraphy characteristics of ATTRv-CA patients are presented in Table 1 and Supplementary Table 1. In the ATTRv-CA group, the patients were predominantly male ($n = 23$, 81%) and elderly (61.5 ± 1.6 years). All patients with ATTRv-CA showed moderate-to-extensive myocardial tracer uptake with VGS ≥ 2 ($n = 28$, 100%) and the mean

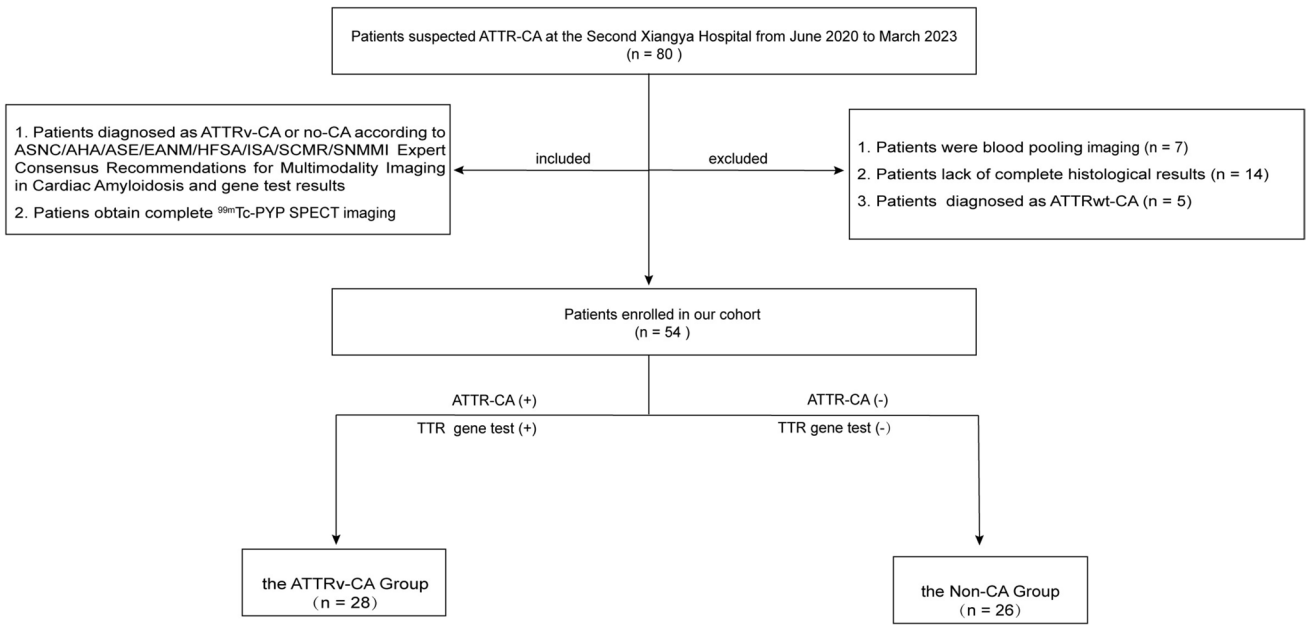

Fig. 1 Patient flowchart in this study group. Eighty patients were recruited for this study. According to the included and excluded criteria, 54 patients were enrolled finally, including 28 ATTRv-CA (ATTRv-CA Group) and 26 non-CA patients (Non-CA Group)

Table 1 Patient characteristics of ^{99m}Tc-PYP scintigraphy

	Non-CA ($n=26$)	ATTRv-CA ($n=28$)	$\chi 2$/Mann–Whitney U test	P value
1-h visual score parameters				
Grade < 2	17 (65)	0 (0)		0.000
Grade ≥ 2	9 (35)	28 (100)		
1-h semiquantitative parameter				
H/CL	1.25 ± 0.03	2.09 ± 0.06	t = 12.328	0.000

Values are mean ± SD, n (%), or median (range); a two-sided P value < 0.050 was considered statistically significant

H/CL ratio was 2.09 ± 0.06. Additionally, eight different genotypes were found in our study: Ala97Ser ($n=13$, 46%), Asp18Asn ($n=4$, 14%), Glu81Lys ($n=3$, 11%), His88Arg ($n=2$, 7%), Thr59Lys ($n=2$, 7%), Ser23Asn ($n=2$, 7%), Arg34Thr ($n=1$, 4%), and Glu74Lys ($n=1$, 4%) (Fig. 2a).

The most common genotype is Ala97Ser, we then divided those 28 ATTRv-CA patients into the Ala97Ser group ($n=13$) and the non-Ala 97Ser group ($n=15$). In the Ala-97Ser group (Table 2), the mean age of disease onset, definite diagnosis, and the median interval between the appearance of symptoms and the actual diagnosis were 61.6 ± 1.9, 66.5 ± 1.3, and 4.0 (3.0–6.2) years, respectively. At the time of diagnosis, amyloidosis involved the myocardium, making a raised myocardial thickness with a mean interventricular septal thickness at diastole (IVSd) of 16.1 ± 0.9 mm on echocardiography and a damaged systolic function with an average left ventricular ejection fraction (LVEF) of 49.6 ± 3.1%. Three clinical sub-phenotypes were ranked according to incidence, including dysfunction of peripheral and autonomic nerves and involvement of other organs. The initial complaint was mostly peripheral nerve dysfunction, mainly characterized by paresthesia (9/13, 69%). Furthermore, autonomic nerve performance, including orthostatic hypotension ($n=3$, 23%), vomiting ($n=2$, 15%), diarrhea ($n=2$, 15%), dysphagia ($n=2$, 15%) and constipation ($n=1$, 8%), and organ involvement manifestations could appear, such as myocardial injury ($n=13$, 100%) and/or others (Supplementary Fig. 1). In ^{99m}Tc-PYP imaging, all Ala97Ser ATTRv-CA patients showed extensive myocardial uptake with VGS = 3, and the H/CL ratio of Ala97Ser group (mean H/CL: 1.95 ± 0.06) is higher than that of the non-Ala97Ser group (mean H/CL: 1.87 ± 0.02), but there was no statistical significance ($p=0.844$).

Diagnostic accuracy and interobserver variability of the visual score

The visual score in the ATTRv-CA group was significantly higher than that in the non-CA group ($p=0.000$) (Table 1). The results indicated significant interobserver variability with an intraclass correlation coefficient of 0.522 for 1-h VGS (95% CI 0.367–0.677, $p<0.001$) (Fig. 3a). When

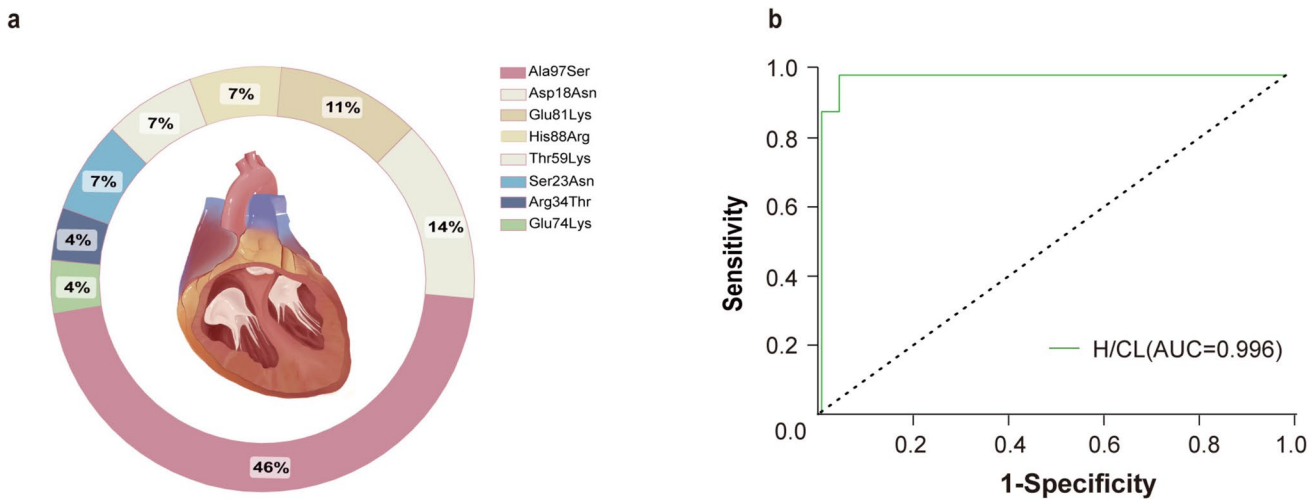

Fig. 2 The details of the TTR-mutated subtype and ROC curve analysis of H/CL ratio. **a** The legend on the top right presents different gene subtypes, and the percentage in the sector of the circle presents the proportion of each gene subtype; **b** ROC curve of H/CL ratio for the diagnosis of ATTRv-CA

Table 2 The comparison between the Ala97Ser and non-Ala97Ser group

Parameters	Ala97Ser group	Non-Ala97Ser group	$\chi 2$/Mann−Whitney *U* test	*P* value
Male, *n* (%)	11 (85)	12 (80)	$\chi 2 = 0.101$	0.750
Initial complaints				
Weight reduction, *n* (%)	1 (8)	0 (0)		
Paresthesia, *n* (%)	9 (69)	6 (40)		
Polypnea, *n* (%)	2 (15)	9 (60)		
Diarrhea, *n* (%)	1 (8)	0 (0)		
Age at diagnosis, years	66.5 ± 1.3	57.00 (52.85, 61.29)	Z = 0.001	0.001
Age of onset, years	61.6 ± 1.9	53.00 (50.14, 59.33)	Z = −2.125	0.025
Interval, years	4.0 (3.0, 6.2)	2.33 ± 0.65	Z = −1.955	0.052
^{99m}Tc-PYP scintigraphy				
1-h visual score parameters				
Grade < 2, n (%)	0 (0)	0 (0)		
Grade ≥ 2, n (%)	13 (100)	15 (100)		
1-h semiquantitative parameter				
H/CL	1.95 ± 0.06	1.87 ± 0.015	t = -0.198	0.844
Echocardiography				
LAS[a], mm	38.08 ± 1.5	39.00 (35.84, 43.08)	Z = -0.437	0.687
RAS[b], mm	39.0 (33.0, 40.9)	37.00 (31.34, 41.12)	Z = -0.361	0.724
RVD[c], mm	31.7 ± 1.5	30.00 (26.94, 31.83)	Z = -1.186	0.243
IVSd[d], mm	16.1 ± 0.9	16.00 (13.91, 17.17)	Z = -0.440	0.687
LVEDd[e], mm	42.4 ± 1.2	45.50 (40.00, 49.50)	Z = 0.372	0.408
LVPWDd[f], mm	14.6 ± 0.8	17.00 (13.97, 17.53)	Z = 0.237	0.247
LVEF[g], %	49.6 ± 3.1	51.00 (45.14, 56.40)	Z = 0.681	0.687

Values are mean ± SD, *n* (%), or median (interquartile range); **a** *LAS* left atrium diameter, **b** *RAS* right atrium diameter, **c** *RVD* right ventricular diameter, **d** *IVSd* interventricular septal thickness on echocardiography, **e** *LVEDd* left ventricular end-diastolic dimension, **f** *LVPWDd* left ventricular posterior wall thickness on echocardiography, **g** *LVEF* left ventricular ejection fraction

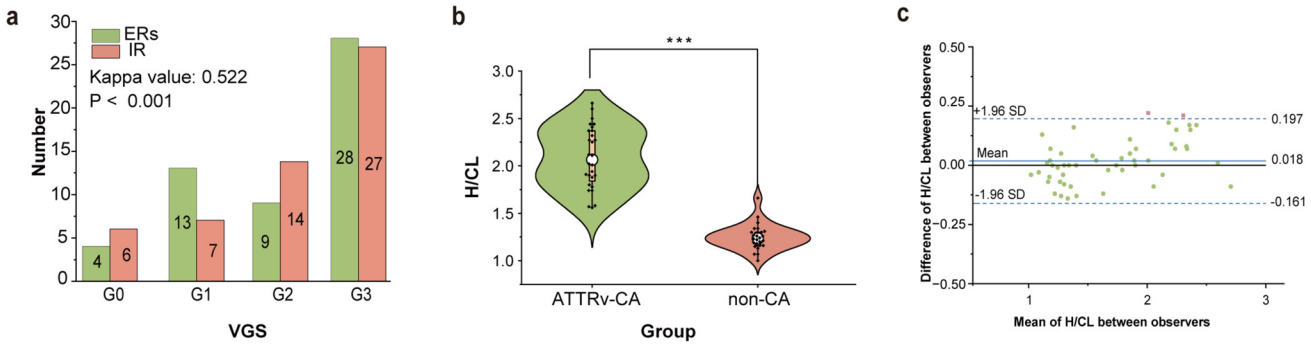

Fig. 3 The distribution and interobserver consistency analysis of VGS and H/CL ratio. **a** Histograms of the visual score among nuclear imaging diagnosticians; the visual score (VGS) among ERs and IR; **b** The H/CL ratio of ATTRv-CA patients was higher than those of the control group ($p < 0.050$); the circle in the box indicates the median value, the box boundary shows the IQR; *** means $p < 0.001$; **c** Bland−Altman plots of nuclear imaging diagnosticians' agreement for H/CL ratio; the solid lines indicate the mean difference among diagnosticians, and the dashed lines indicate the limits of agreement (1.96 SDs of the mean difference); the pink squares indicate points outside the interval, and the blue dots represent points in the interval

employing VGS ≥ 2 as the positive diagnosis criterion, we found that all ATTRv-CA patients were positive. In contrast, nine non-CA patients also showed false-positive results, which resulted in high sensitivity (100%) but low specificity (65%).

Diagnostic accuracy and interobserver variability of the semiquantitative parameter (H/CL ratio)

The mean H/CL ratio of ATTRv-CA was 2.09 ± 0.06, which was significantly higher than those of the non-CA group (Table 1; Fig. 3b). The receiver operating characteristic (ROC) curve analysis confirmed that the semiquantitative parameter, H/CL ratio, showed high diagnostic values (Fig. 2b). The area under the ROC curve (AUC) of H/CL was 0.996 (Se: 100%, Sp: 96%, cutoff value: 1.51, 95% CI 0.986–1.000; $p = 0.000$). Moreover, Bland−Altman analysis indicated high interobserver consistency of H/CL among diagnosticians (Fig. 3c). The mean difference in H/CL among diagnosticians was 0.018, and the 95% limit of agreement ranged from −0.161 to 0.197.

Correlational analyses among the H/CL and NAC stage, echocardiographic-related parameters, or blood biomarkers

We further performed correlational analyses between semiquantitative parameter (H/CL ratio) of ATTRv-CA patients and NAC stage, echocardiographic-related parameters, or blood biomarkers. The results showed that the H/CL ratio exhibited no significant difference or correlation between NAC stage I (mean H/CL ratio: 2.00 ± 0.08) and NAC stage II (mean H/CL ratio: 2.19 ± 0.08) patients ($p = 0.042$) (Supplementary Fig. 2). Additionally, echocardiographic-related parameters or blood biomarkers had no significant correlations with the H/CL ratio ($p > 0.05$) (Supplementary Fig. 3).

Discussion

Different *TTR*-mutated genotypes exhibit varied clinical manifestations, disease progression, and distribution characteristics [6]. For example, the Val30Met (p. Val50Met) variant is a late-onset disease [3] that is responsible for the high prevalence of ATTRv-CA in endemic areas [23, 24] such as Portugal, Sweden and Japan, and it tends to include less severe cardiac involvement with positive ^{99m}Tc-PYP scintigraphy results compared to individuals with the same mutation, but from a nonendemic area or individuals with non-Val30Met mutations [25]. Phe64Leu mutation-related transthyretin cardiac amyloidosis is the most common mutation in southern Italy [24]. The clinical characteristic of this genotype has not been systematically summarized. A multicenter study revealed that bone scintigraphy has low sensitivity in detecting Phe64Leu mutation-related transthyretin cardiac amyloidosis [26]. Ala97Ser mutation is a relatively common reported subtype in China, Malaysia and Thailand [27–29], with characteristics of later onset, rapid progression and lack of specific features [30]. The application of bone scintigraphy in diagnosing ATTRv-CA has received less attention. There is an urgent need to assess the diagnostic accuracy of bone scintigraphy across a wider spectrum of *TTR* mutations in different geographic areas. Therefore, this study demonstrated an understanding of the features of *TTR* gene mutations in our center, especially the most populated Ala97Ser sub-genotype of our center, and compared the diagnostic accuracy of the visual score and semiquantitative parameter of ^{99m}Tc-PYP scintigraphy in the diagnosis of ATTRv-CA.

Ala97ser is a kind of later-onset and rapidly progressive, but delayed diagnostic genotype

The most populated genotype was Ala97Ser in our cohort. It is a kind of later-onset rapidly progressive genotype that lacks specific features at the initial stage to enable differentiation from other genotypes [30]. In addition, Ala97Ser gene-mutated patients in our cohort who had cardiac involvement manifested chest distress and shortness of breath, lower limb edema, syncope, and a thickened left ventricular wall on ultrasonography. These nonspecific features make it difficult to distinguish it from other cardiomyopathies [31], such as hypertrophic heart disease. Therefore, noninvasive imaging with higher specificity is needed to improve the diagnostic rate. Fortunately, ^{99m}Tc-PYP scintigraphy meets this requirement completely from our research results. Those patients' visual scores are Grade 3, and the mean H/CL ratio is 1.95 ± 0.06, corresponding to the current ^{99m}Tc-PYP positive diagnostic criteria. But no statistical significance exists in the H/CL ratio between the Ala97Ser and non-Ala97Ser group. With the varied characteristics of different genotypes in the non-Ala97Ser group, the difference of H/CL ratio between different genotype need separate comparison. We will continue to collect different genotypes and make further detailed sub-genotype analysis.

Semiquantitative parameter (H/CL) is more useful than visual score in the diagnosis of ATTRv-CA

One of the most common visual score criteria is comparing the relative uptake between the heart and ribs. VGS ≥ 2 is considered one of the positive criteria to make an ATTR-CA diagnosis [31]. However, Poterucha et al. [8] noted that nearly two-thirds of VGS ≥ 2 results in their center were false positive; similar results also repeatedly emerged at other research centers, which indicated that VGS ≥ 2

possesses a fatal flaw of subjectivity [32, 33] and that the visual score is not reliable enough to diagnose ATTR-CA [11, 21]. Thus, we evaluated the diagnostic efficiency of the visual score at 1-h postinjection at our center. The results showed that the interobserver consistency of a 1-h visual score was significantly different among diagnosticians, and a high false-positive rate was observed when applying VGS ≥ 2 as a positive diagnostic criterion. Although most of the H/CL values of the non-CA patients were lower than 1.51, 35% ($n = 9$) of patients had a visual score ≥ 2, which puzzles nuclear medicine diagnosticians when judging the image and might cause a misdiagnosis. The results showed that the semiquantitative criteria, H/CL ratio, is more useful than VGS in the diagnosis of ATTRv-CA. One of the reasons for this inferior diagnostic accuracy of visual score might be attributable to the use of the 1-h image instead of the 3-h image. The 1-h planar ^{99m}Tc-PYP images showed high sensitivity, while 3-h planar ^{99m}Tc-PYP images showed high specificity for the diagnosis of ATTR-CA [34]. However, with the limitation of the retrospective study, 3-h planar imaging data is unavailable. We will develop a prospective study to make further comparisons about the diagnostic efficiency of visual score and H/CL ratio in 1-h and 3-h planar and SPECT imaging.

The current recommended semiquantitative parameter for the diagnosis of CA is H/CL. Although H/CL is highly reproducible in different study centers, a study has mentioned high misdiagnosis rates [8]. Our results indicated that the delineated semiquantitative parameter, H/CL ratio, obtained high diagnostic efficiency and interobserver consistency for diagnosing ATTRv-CA. In our study center, the average H/CL ratio was significantly different between these two groups, and the H/CL ratios in the ATTRv-CA group (mean H/CL: 2.09 ± 0.06) were higher than those in the non-CA group (mean H/CL: 1.25 ± 0.03). This means that ^{99m}Tc-PYP scintigraphy obtains high diagnostic accuracy that could primarily distinguish ATTRv-CA patients from non-ATTRv-CA patients after excluding other types of CA (such as AL-CA and ATTRwt-CA). However, as ATTRwt-CA usually manifests in old age, patients usually recognize that symptoms are the results of aging and diminishing organ function and so rarely seek medical attention [2, 29]. As a result, ATTRv-CA ($n = 28$) is well represented and ATTRwt-CA ($n = 5$) is less prevalent in our cohort. We further analyzed the semiquantitative parameter (H/CL) between ATTRwt-CA and ATTRv-CA patients. We found that although the H/CL ratio of ATTRv-CA) is higher than that of ATTRwt-CA patients [mean H/CL: 2.09 ± 0.06 vs. 1.74 (1.46, 2.29)], no statistical significance exists ($p = 0.173$) (Supplementary Table 3). The small cohort of ATTRwt-CA might a significant contribution. Thus, a large and multicenter study is warranted to make a further comparison.

Study limitations

The limitations in this paper are principally due to the retrospective design of this study. First, this was a selected cohort in which there was a high pretest probability for ATTR-CA, and its relevance to populations with a lower pretest probability is uncertain. A larger, multicenter study is needed to verify our conclusion. Additionally, because of the scattered genotype distribution, we cannot determine the similarities and differences of various gene mutations. We will continue to explore the specificity of ^{99m}Tc-PYP scintigraphy in diagnosing ATTRv-CA.

Conclusion

The Ala97Ser gene mutation accounted for a large proportion of ATTRv-CA in our cohort, with characteristics of later onset and rapid disease progression, but delayed diagnosis. ^{99m}Tc-PYP scintigraphy indicated high diagnostic value in 13 Ala97Ser gene-mutated patients with intensive myocardial uptake. Additionally, ^{99m}Tc-PYP scintigraphy obtains high diagnostic efficiency in the diagnosis of ATTRv-CA. The semiquantitative parameter, H/CL ratio (cutoff value: 1.51), is more useful in the diagnosis of ATTRv-CA than visual score.

Supplementary Information The online version contains supplementary material available at https://doi.org/10.1007/s12149-023-01898-x.

Acknowledgements We express our appreciation to Mrs. Alisa Rogoff from the USA for language editing of the manuscript. The authors declare that the research was conducted without any commercial or financial relationships that could be construed as potential conflicts of interest.

Funding This work was supported by a significant grant from the Research and Development Program of Hunan Province of China (2019SK2252, 2022SK2035) and the Natural Science Foundation of Hunan Province of China (2020JJ4801).

Data availability Data are available on request to the first author.

References

1. Alexander KM, Masri A. Recipe for success in transthyretin cardiomyopathy: monoclonal protein rule out, SPECT imaging, and genetic testing. JACC Cardiovasc Imaging. 2021;14:1232–4.
2. Castaño A, Narotsky DL, Hamid N, Khalique OK, Morgenstern R, DeLuca A, et al. Unveiling transthyretin cardiac amyloidosis and its predictors among elderly patients with severe aortic stenosis undergoing transcatheter aortic valve replacement. Eur Heart J. 2017;38:2879–87.
3. Ruberg FL, Berk JL. Transthyretin (TTR) cardiac amyloidosis. Circulation. 2012;126:1286–300.

4. Benson MD, Buxbaum JN, Eisenberg DS, Merlini G, Saraiva MJM, Sekijima Y, et al. Amyloid nomenclature 2020: update and recommendations by the International Society of Amyloidosis (ISA) nomenclature committee. Amyloid. 2020;27:217–22.
5. Sekijima Y. Transthyretin (ATTR) amyloidosis: clinical spectrum, molecular pathogenesis and disease-modifying treatments. J Neurol Neurosurg Psychiatry. 2015;86:1036–43.
6. Haq M, Pawar S, Berk JL, Miller EJ, Ruberg FL. Can 99mTc-pyrophosphate aid in early detection of cardiac involvement in asymptomatic variant TTR amyloidosis? JACC Cardiovasc Imaging. 2017;10:713–4.
7. Hsueh H-W, Chao C-C, Chang K, Jeng Y-M, Katsuno M, Koike H, et al. Unique phenotypes with corresponding pathology in late-onset hereditary transthyretin amyloidosis of A97S vs. V30M. Front Aging Neurosci. 2021;13:786322.
8. Poterucha TJ, Elias P, Bokhari S, Einstein AJ, DeLuca A, Kinkhabwala M, et al. Diagnosing transthyretin cardiac amyloidosis by technetium Tc 99m pyrophosphate: a test in evolution. JACC Cardiovasc Imaging. 2021;14:1221–31.
9. Merlo M, Porcari A, Pagura L, Cameli M, Vergaro G, Musumeci B, et al. A national survey on prevalence of possible echocardiographic red flags of amyloid cardiomyopathy in consecutive patients undergoing routine echocardiography: study design and patients characterization - the first insight from the AC-TIVE Study. Eur J Prev Cardiol. 2022;29:e173–7.
10. Merlo M, Pagura L, Porcari A, Cameli M, Vergaro G, Musumeci B, et al. Unmasking the prevalence of amyloid cardiomyopathy in the real world: results from phase 2 of AC-TIVE study, an Italian Nationwide survey. Eur J Heart Fail. 2022;24(8):1377–86.
11. Ayers MP, Peruri AV, Bourque JM. Nonbiopsy diagnosis of cardiac transthyretin amyloidosis. J Nucl Cardiol. 2021;28:1846–50.
12. Gillmore JD, Maurer MS, Falk RH, Merlini G, Damy T, Dispenzieri A, et al. Expert consensus recommendations for the suspicion and diagnosis of transthyretin cardiac amyloidosis. Circulation. 2016;133:2404–12.
13. Garcia-Pavia P, Rapezzi C, Adler Y, Arad M, Basso C, Brucato A, et al. Diagnosis and treatment of cardiac amyloidosis: a position statement of the ESC Working Group on Myocardial and Pericardial Diseases. Eur Heart J. 2021;42:1554–68.
14. Dorbala S, Ando Y, Bokhari S, Dispenzieri A, Falk RH, Ferrari VA, et al. ASNC/AHA/ASE/EANM/HFSA/ISA/SCMR/SNMMI expert consensus recommendations for multimodality imaging in cardiac amyloidosis: Part 1 of 2-evidence base and standardized methods of imaging. Circ Cardiovasc Imaging. 2021;14: e000029.
15. Maurer MS. Noninvasive identification of ATTRwt cardiac amyloid: the re-emergence of nuclear cardiology. Am J Med. 2015;128:1275–80.
16. Carroll A, Dyck PJ, de Carvalho M, Kennerson M, Reilly MM, Kiernan MC, et al. Novel approaches to diagnosis and management of hereditary transthyretin amyloidosis. J Neurol Neurosurg Psychiatry. 2022;93:668–78.
17. Dorbala S, Ando Y, Bokhari S, Dispenzieri A, Falk RH, Ferrari VA, et al. ASNC/AHA/ASE/EANM/HFSA/ISA/SCMR/SNMMI expert consensus recommendations for multimodality imaging in cardiac amyloidosis: part 2 of 2-diagnostic criteria and appropriate utilization. Circ Cardiovasc Imaging. 2021;14: e000030.
18. Bokhari S, Morgenstern R, Weinberg R, Kinkhabwala M, Panagiotou D, Castano A, et al. Standardization of 99mTechnetium pyrophosphate imaging methodology to diagnose TTR cardiac amyloidosis. J Nucl Cardiol. 2018;25:181–90.
19. Sperry BW, Bateman TM, Akin EA, Bravo PE, Chen W, Dilsizian V, et al. Hot Spot Imaging in Cardiovascular Diseases: An Information Statement from SNMMI, ASNC, and EANM. J Nucl Med. 2022;jnumed.122.264311.
20. Sperry BW, Burgett E, Bybee KA, McGhie AI, O'Keefe JH, Saeed IM, et al. Technetium pyrophosphate nuclear scintigraphy for cardiac amyloidosis: Imaging at 1 vs 3 hours and planar vs SPECT/CT. J Nucl Cardiol. 2020;27:1802–7.
21. Bokhari S, Castaño A, Pozniakoff T, Deslisle S, Latif F, Maurer MS. (99m)Tc-pyrophosphate scintigraphy for differentiating light-chain cardiac amyloidosis from the transthyretin-related familial and senile cardiac amyloidoses. Circ Cardiovasc Imaging. 2013;6:195–201.
22. Law S, Bezard M, Petrie A, Chacko L, Cohen OC, Ravichandran S, et al. Characteristics and natural history of early-stage cardiac transthyretin amyloidosis. Eur Heart J. 2022;43:2622–32.
23. Rowczenio DM, Noor I, Gillmore JD, Lachmann HJ, Whelan C, Hawkins PN, et al. Online registry for mutations in hereditary amyloidosis including nomenclature recommendations. Hum Mutat. 2014;35:E2403–12.
24. Russo M, Obici L, Bartolomei I, Cappelli F, Luigetti M, Fenu S, et al. ATTRv amyloidosis Italian registry: clinical and epidemiological data. Amyloid. 2020;27:259–65.
25. Rapezzi C, Longhi S, Milandri A, Lorenzini M, Gagliardi C, Gallelli I, et al. Cardiac involvement in hereditary-transthyretin related amyloidosis. Amyloid. 2012;19(Suppl 1):16–21.
26. Musumeci MB, Cappelli F, Russo D, Tini G, Canepa M, Milandri A, et al. Low sensitivity of bone scintigraphy in detecting Phe64Leu mutation-related transthyretin cardiac amyloidosis. JACC Cardiovasc Imaging. 2020;13:1314–21.
27. Chou CT, Lee CC, Chang DM, Buxbaum JN, Jacobson DR. Familial amyloidosis in one Chinese family: clinical, immunological, and molecular genetic analysis. J Intern Med. 1997;241:327–31.
28. Chou CT, Lee CC, Chang DM, Buxbaum JN, Jacobson DR. Transthyretin Ala97Ser is associated with familial amyloidotic polyneuropathy in a Chinese-Taiwanese family. J Intern Med. 1997;241:327–31.
29. Yu A-L, Chen Y-C, Tsai C-H, Chao C-C, Su M-Y, Juang JJ-M, et al. Tafamidis treatment decreases 99mTc-pyrophosphate uptake in patients with hereditary Ala97Ser transthyretin amyloid cardiomyopathy. JACC Cardiovasc Imaging. 2023;16:866–7.
30. Ungerer MN, Hund E, Purrucker JC, Huber L, Kimmich C, Aus dem Siepen F, et al. Real-world outcomes in non-endemic hereditary transthyretin amyloidosis with polyneuropathy: a 20-year German single-referral centre experience. Amyloid. 2021;28:91–9.
31. Ayers MP, Peruri AV, Bourque JM. Transforming ATTR cardiac amyloidosis into a chronic disease: The enormous potential of quantitative SPECT to improve diagnosis, prognosis, and monitoring of disease progression. J Nucl Cardiol. 2021;28:1846–50.
32. Masri A, Bukhari S, Ahmad S, Nieves R, Eisele YS, Follansbee W, et al. Efficient 1-hour technetium-99 m pyrophosphate imaging protocol for the diagnosis of transthyretin cardiac amyloidosis. Circ Cardiovasc Imaging. 2020;13: e010249.
33. Sperry BW, Vranian MN, Tower-Rader A, Hachamovitch R, Hanna M, Brunken R, et al. Regional variation in technetium pyrophosphate uptake in transthyretin cardiac amyloidosis and impact on mortality. JACC Cardiovasc Imaging. 2018;11:234–42.
34. Castano A, Haq M, Narotsky DL, Goldsmith J, Weinberg RL, Morgenstern R, et al. Multicenter study of planar technetium 99m pyrophosphate cardiac imaging: predicting survival for patients with ATTR cardiac amyloidosis. JAMA Cardiol. 2016;1:880–9.